

PCCP

Accepted Manuscript



This is an *Accepted Manuscript*, which has been through the Royal Society of Chemistry peer review process and has been accepted for publication.

Accepted Manuscripts are published online shortly after acceptance, before technical editing, formatting and proof reading. Using this free service, authors can make their results available to the community, in citable form, before we publish the edited article. We will replace this *Accepted Manuscript* with the edited and formatted *Advance Article* as soon as it is available.

You can find more information about *Accepted Manuscripts* in the [Information for Authors](#).

Please note that technical editing may introduce minor changes to the text and/or graphics, which may alter content. The journal's standard [Terms & Conditions](#) and the [Ethical guidelines](#) still apply. In no event shall the Royal Society of Chemistry be held responsible for any errors or omissions in this *Accepted Manuscript* or any consequences arising from the use of any information it contains.

Characteristics of fast mediated bioelectrocatalytic reaction near micro-electrodes

Yuki Kitazumi,^{*a,c} Tatsuo Noda,^{a‡}, Osamu Shirai,^a, Masahiro Yamamoto,^{*b,c}, and Kenji Kano^{a,c}

Received Xth XXXXXXXXXXXX 20XX, Accepted Xth XXXXXXXXXXXX 20XX

First published on the web Xth XXXXXXXXXXXX 200X

DOI: 10.1039/b000000x

The pseudo-steady-state current due to a mediated enzymatic reaction on a microelectrode is characterized on the basis of theoretical analysis and numerical simulation. The steady-state current is proportional to substrate concentration when the enzymatic reaction is considerably faster than substrate mass transport via nonlinear diffusion. Under such conditions, the reaction plane, where the mass flow of the substrate is converted to that of the mediator, exists near the electrode surface. The steady-state current increases as the diffusion coefficient of the substrate increases. In contrast, the diffusion coefficient and the concentration of the mediator have minor effects on the current. This difference can be explained on the basis of a change in the reaction plane location. When a sufficient amount of enzyme exists in a system, the system can be used as an amperometric biosensor, the response of which is independent of any change in enzyme activity.

1 Introduction

Bioelectrocatalytic reactions, a conjugation of biocatalysis by enzymes and electrode reaction, lead to high enzyme selectivity in electrochemical devices, thereby offering benefits in terms of handling and sensitivity. Thus, the combination of an electrochemical devices and an enzymatic reaction is frequently used as an electrochemical biosensor.^{1–5} Electrochemical biosensors are classified into three generations. In first-generation biosensors, the product of the enzymatic reaction is detected electrochemically. Second-generation biosensors employ a mediator for connecting the enzymatic reaction with the electrode. In third-generation biosensors, direct electron transfer takes place between the enzyme and the electrode. Among these sensor generations, the second-generation sensors, i.e., mediated enzymatic reaction-based sensors, afford the highest levels of flexibility in system design.^{2,3} Three electrochemical methods, amperometry, coulometry, and potentiometry, are employed for detecting whether the mediator reacted with the substrate. In these methods, amperometry offers the best balance of the detection time, accuracy, and usability.

However, when the current response of an amperometric

sensor is time dependent, its practical application is limited. Steady-state current is necessary for stable amperometric sensors. One of the ideas is the use of microelectrode detection. Nonlinear diffusion of the substrate around the microelectrode results in mass transfer that is adequate for sustaining a steady-state current.^{6,7} Additionally, the use of a microelectrode is effective from the viewpoint of biosensor miniaturization.^{8,9} In contrast, the enzymatic electrode reaction provides a steady-state current when the mass transfer due to substrate diffusion is balanced with the rate of enzymatic reaction.¹⁰ The physical meaning of the steady-state current obtained using the combination of nonlinear diffusion and rate of enzymatic electrode reaction is complicated, because the two mechanisms compete with each other for control of the current. The enzymatic electrode reaction-microelectrode combination finds limited application in endpoint analysis.¹¹

Recently, our group investigated a mediated enzymatic electrode reaction on a microdisc electrode, which provides a pseudo-steady-state current that is practically proportional to the substrate concentration.¹² In this system, the apparent enzymatic reaction rate is set to be extremely fast by increasing the enzyme concentration. For characterizing the linear response of the steady-state current to the substrate concentration for general application as an ultimate biosensor, a model incorporating nonlinear diffusion and an enzymatic reaction is necessary for analyzing the current response of a mediated enzymatic electrode reaction on a microdisc electrode. The current at the microdisc electrode collaborated with the enzymatic reaction has been tackled by Galceran et al.¹³ Furthermore, the current at a micro spherical electrode under a homogeneous catalytic reaction was analyzed and calculated

^a Division of Applied Life Sciences, Graduate School of Agriculture, Kyoto University, Sakyo, Kyoto, 606-8502, Japan. Fax: +81-75-753-6456; Tel: +81-75-753-6393; E-mail: kitazumi.yuki.7u@kyoto-u.ac.jp

^b Department of Chemistry, Konan University, 8-9-1 Okamoto, Higashi-Nada, Kobe, Hyogo, 658-8501, Japan. Fax: +81-78-435-2497; Tel: +81-78-435-2497; E-mail: masahiro@konan-u.ac.jp

^c Core Research for Evolutional Science and Technology (CREST), Japan Science and Technology Agency

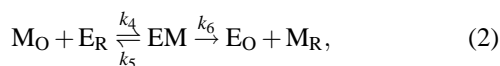
[‡] Present address: Osaka Prefecture University College of Technology, Osaka, Osaka, 572-8572, Japan

numerically by Eswari and Rajendran.^{14,15} However, their calculations were performed under slow catalytic reaction conditions, and it is difficult to extend the result (or prediction) to the system assumed here.¹²

In this work, the current produced by a mediated bioelectrocatalytic reaction on a microdisc electrode with an extremely fast enzymatic reaction rate is investigated with a simplified mathematical model and numerical simulation. The calculations indicate the advantages of this system from the practical application viewpoint.

2 Analytical model

A reaction-diffusion model is introduced for analytically determining the current produced by the enzymatic microelectrode reaction. For simplifying the mathematical treatment of the microelectrode system, spherical coordinates are introduced, and a semispherical microelectrode is considered. A schematic view of the microelectrode is shown in Fig. 1A. The radius of the microelectrode is denoted by r_0 . A hemisphere with the radius r_1 is the reaction plane where the enzymatic reaction occurs under the steady-state condition (our simulation, described later, validates the reasonability of this reaction plane assumption). Here, we assume an oxidative reaction of the substrate (S, as a reductant), and in the beginning, S, the oxidized enzyme (E_O), and the oxidized mediator (M_O) are assumed to be added in the system at the analytical concentrations of c_S^0 , c_M^0 , and c_E^0 , respectively. In the solution phase, the enzymatic reactions proceed as below.



where the subscripts R and O denote the reduced and oxidized forms, respectively, ES and EM indicate the Michaelis complexes, and k_i on the arrows represents the reaction rate constants. The redox reaction of the mediator occurs on the electrode surface.



Under the limiting current conditions, M_R is completely oxidized on the electrode surface. The boundary conditions are formulated as follows:

$$c_{M_R}(r_0) = 0 \quad (4)$$

and

$$c_{M_O}(r_0) = c_M^0, \quad (5)$$

where c_M^0 is equal to the total mediator concentration in the system. An extremely fast enzymatic reaction is assumed

here. M_O will be completely reduced by S near the electrode at the position of r_1 . Under the steady-state conditions, this assumption implies that the inflow flux of S (J_S) across the reaction plane surface is completely converted to the inflow flux of M_R (J_{M_R}). Therefore, the value of $2\pi r_1^2 J_S$ is equal to the oxidation rate of M_R on the electrode surface.

The concentration and flux profiles around the spherical electrode under the limiting current conditions are written as follows:

$$c(r) = \Delta c \left(1 - \frac{r_0}{r}\right) \quad (6)$$

and

$$J(r) = -D \frac{\partial c(r)}{\partial r} = -\frac{D\Delta c r_0}{r^2}, \quad (7)$$

where Δc denotes the concentration difference between in the bulk phase and that on the electrode surface. Therefore, the profile of J_S outside the reaction plane is written as follows:

$$J_S(r) = -D_S \frac{\partial c_S(r)}{\partial r} = -D_S (c_S(\infty) - c_S(r_1)) \frac{r_1}{r^2}, \quad (8)$$

where $c_S(\infty)$ denotes the bulk concentration of S and D_S denotes the diffusion coefficient of S. The concentration profile of S is written as

$$c_S(r) = c_S(\infty) - c_S(r_1) - \frac{r_1 (c_S(\infty) - c_S(r_1))}{r}. \quad (9)$$

According to the given conditions, when $c_S^0 \gg c_M^0 + c_E^0$, S in the bulk phase is oxidized by M_O and E_O , and $c_S(\infty)$ is written as

$$c_S(\infty) = c_S^0 - c_M^0 - c_E^0 \simeq c_S^0 - c_M^0. \quad (10)$$

Thus, the profiles of J_{M_R} and c_{M_R} inside the reaction plane are written as

$$J_{M_R}(r) = -D_M \frac{\partial c_{M_R}(r)}{\partial r} = -D_M \frac{c_{M_R}(r_1) r_1}{r_1 - r_0} \frac{r_0}{r^2} \quad (11)$$

and

$$c_{M_R}(r) = \frac{c_{M_R}(r_1) r_1}{r_1 - r_0} \left(1 - \frac{r_0}{r}\right), \quad (12)$$

respectively, where D_M is the diffusion coefficient of the mediator.

Here, additionally, our model assumes that $c_{M_R}(r_1)$ is equal to c_M^0 . The steady-state current (I_d) is written as follows:

$$I_d = -2\pi n F D_M \frac{c_M^0 r_0 r_1}{r_1 - r_0} \quad (13)$$

$$= 2\pi n F D_S (c_S^0 - c_M^0 - c_E^0 - c_S(r_1)) r_1. \quad (14)$$

This model requires the definition of r_1 and $c_S(r_1)$ for calculating the current. If the enzymatic reaction is extremely fast, r_1 and $c_S(r_1)$ will converge to r_0 and 0, respectively. Moreover,

c_E^0 can be decreased to 0. Under these limiting conditions, eq. 14 is written as

$$I_d = 2\pi nFD_S(c_S^0 - c_{M_O}^0)r_0 \quad (15)$$

$$\simeq 2\pi nFD_S c_S^0 r_0 \quad (16)$$

This situation agrees with the diffusion-limited condition of S at the electrode surface.

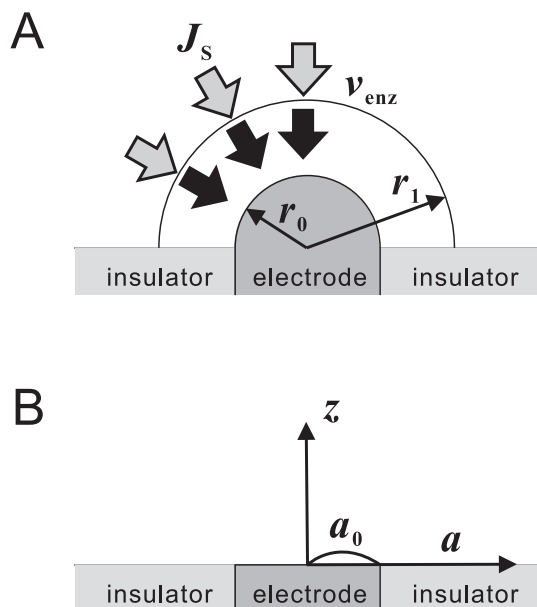


Fig. 1 Geometries of (A) the theoretical model of enzymatic reaction at a micro hemisphere electrode and (B) the numerical simulation around the microdisc electrode.

3 Numerical simulation

For characterizing the system without assumption of the reaction plane used in the simplified mathematical model, a numerical simulation is carried out. In this calculation, the diffusion equations of S, M_O, and M_R are considered. The diffusion of the enzyme derivatives (E_R, E_O, E_M, and E_S) can be ignored because these species are huge and their diffusion coefficients will be extremely smaller than those of the other relevant small molecules. The microdisc electrode used in this model (Fig. 1B) has a radius (a_0) of 25 μm , as in a previously reported experimental condition.¹² The rate of the mediator redox reaction on the electrode surface is determined using the Butler-Volmer equation. The parameter values employed are $n = 1$, $T = 298.2 \text{ K}$, $k_1 = 1.0 \times 10^3 \text{ m}^3 \text{ mol}^{-1} \text{ s}^{-1}$, $k_2 = 1.0 \times 10^2 \text{ s}^{-1}$, $k_3 = 1.0 \times 10^5 \text{ s}^{-1}$, $k_4 = 3.0 \times 10^6 \text{ m}^3 \text{ mol}^{-1} \text{ s}^{-1}$, $k_5 = 2.0 \times 10^4 \text{ s}^{-1}$, $k_6 = 1.0 \times 10^5 \text{ s}^{-1}$,^{12,16} $\alpha = 0.5$, and $k^0 = 1.0 \text{ s}^{-1}$, where k^0 , n , T , α , and E^0 are the

standard rate constant of the Butler-Volmer equation, number of electrons, temperature, transfer coefficient, and formal potential of the mediator redox reaction.

The current is determined by integrating as follows at the electrode surface:

$$I = \int_0^{a_0} 2\pi nFD_{M_a} \frac{\partial c_{M_R}}{\partial z} da, \quad (17)$$

where z is the coordinate parallel to the rotation axis.

Potential-step measurements are simulated by changing the boundary condition at the electrode surface. The potential at the electrode surface is stepped from -200 mV to 200 mV against E^0 .

Three reaction-diffusion equations written as follows

$$\frac{\partial c_{M_R}}{\partial t} = D_M \nabla^2 c_{M_R} + k_6 c_{EM}, \quad (18)$$

$$\frac{\partial c_{M_O}}{\partial t} = D_M \nabla^2 c_{M_O} - k_4 c_{M_O} c_{E_R} + k_5 c_{EM}, \quad (19)$$

and

$$\frac{\partial c_S}{\partial t} = D_S \nabla^2 c_S - k_1 c_S c_{E_O} + k_2 c_{ES} \quad (20)$$

and four kinetic equations for E_R, E_O, E_S, and E_M are solved using the finite element method. Calculations are carried out using commercial FEM package called COMSOL 4.3b (COMSOL) on a workstation equipped with two Intel Xeon processors and 64 GByte RAM.

4 Results and discussion

4.1 Current time response

Figure 2 shows the calculated chronoamperograms at $c_S^0 =$ (solid line) 5, (broken line) 10, and (dotted line) 15 mmol dm^{-3} . These amperograms corresponds to the typical time courses of potential-step amperometric measurements at the microdisc electrode. The theoretical current-time response at the microdisc electrode when the potential is stepped to the limited current region has been derived by Shoup and Szabo as follows:¹⁷

$$i = 4nFDc_b a_0 \left(0.7854 + 0.8862\tau^{-1/2} + 0.2146e^{-0.7823\tau^{-1/2}} \right), \quad (21)$$

where $\tau = 4Dt/a_0^2$, c_b denotes the redox species' bulk concentration, and D denotes the redox species' diffusion coefficient. The circles in Fig. 2 show the current estimated using eq. 21 when $D_S = 6.0 \times 10^{-10} \text{ m}^2 \text{ s}^{-1}$ and $c_b = c_S^0 - c_{M_O}^0 - c_{E_O}^0 = 3.8 \text{ mmol dm}^{-3}$. The numerically simulated current at $c_S^0 = 5 \text{ mmol dm}^{-3}$ agrees well with the circles. This shows that the simulated current is almost controlled by the diffusion of S. The small deviation is ascribed to the kinetic resistance because of the enzymatic reaction.

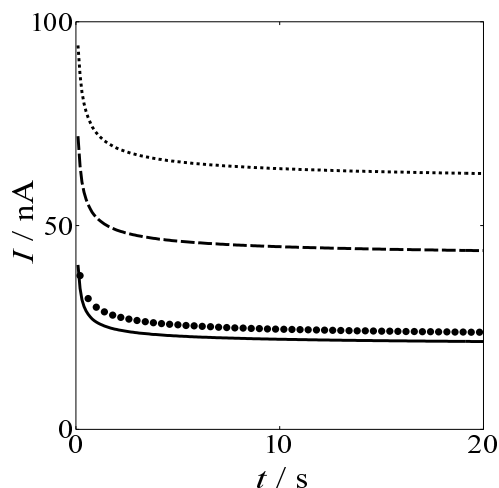


Fig. 2 Chronoamperograms of catalytic current on microdisc electrode at $c_S^0 =$ (solid line) 5, (broken line) 10, and (dotted line) 15 mmol dm^{-3} , $c_E^0 = 0.2 \text{ mmol dm}^{-3}$, $c_M^0 = 1 \text{ mmol dm}^{-3}$, $D_M = 1 \times 10^{-10} \text{ m}^2 \text{ s}^{-1}$, and $D_S = 6 \times 10^{-10} \text{ m}^2 \text{ s}^{-1}$. Circles indicate the current calculated using eq. 21 at $c_b = 3.8 \text{ mmol dm}^{-3}$ and $D = 6 \times 10^{-10} \text{ m}^2 \text{ s}^{-1}$.

The true steady-state current of the microdisc electrode (I_{SS}) is given by¹⁸

$$I_{SS} = 4nFDc_b a_0. \quad (22)$$

At 20 s after the potential step, the current (I_{20}) is in an almost steady-state, but it is 8 percent larger than I_{SS} (at $D_S = 6 \times 10^{-10} \text{ m}^2 \text{ s}^{-1}$). Because the time dependence of I_{20} is practically ignored in practical sensing performance, I_{20} is regarded as the steady-state current in this paper.

4.2 Concentration profiles around electrode

Figure 3 shows the concentration profiles of (A) S, (B) M_R , and (C) E_R near the electrode recorded 20 s after the potential step at $c_M^0 = 1 \text{ mmol dm}^{-3}$, $c_E^0 = 0.2 \text{ mmol dm}^{-3}$, and $c_S^0 = 4 \text{ mmol dm}^{-3}$. The color-filled part of the scaled bar indicates the concentration. The c_S is nearly radially distributed. This shows the distribution of c_S is controlled by the hemispherical diffusion as if S is removed at the electrode surface. However, the concentration gradients of c_{M_R} and c_{E_R} exist only in the vicinity of the electrode. At the electrode surface, M_R is completely oxidized and M_O in the bulk phase is completely reduced by the enzymatic reaction with S. Therefore, in the bulk phase, c_{M_R} is practically zero and c_{M_R} is equal to the value of c_M^0 . The oxidation of M_R at the electrode induces the diffusion of M_R from the bulk phase. The regeneration of M_R in the solution phase determines the reaction plane position.

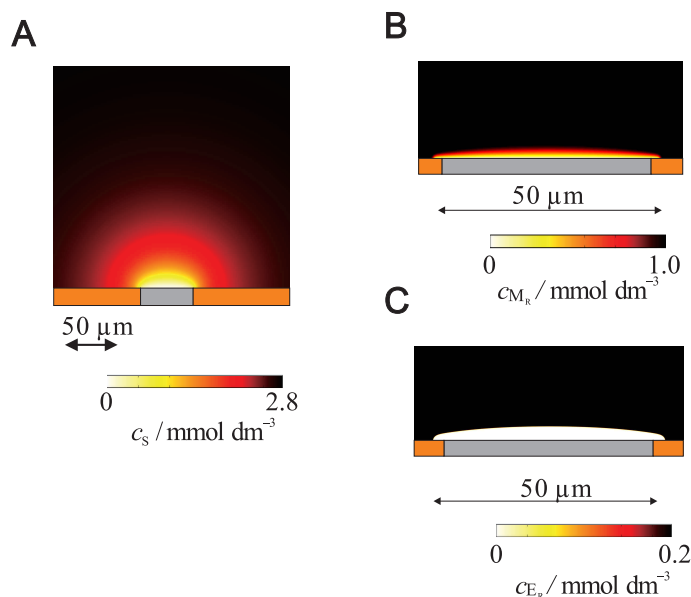


Fig. 3 Cross-sectional view of concentration profiles of (A) substrate (S), (B) reduced mediator (M_R), and (C) reduced form of enzyme (E_R) around a microelectrode at $c_S^0 = 4 \text{ mmol dm}^{-3}$, $c_M^0 = 1 \text{ mmol dm}^{-3}$, $c_E^0 = 0.2 \text{ mmol dm}^{-3}$, $D_S^0 = 6 \times 10^{-10} \text{ m}^2 \text{ s}^{-1}$, and $D_M^0 = 1 \times 10^{-10} \text{ m}^2 \text{ s}^{-1}$. The profiles were recorded 20 s after the potential step.

Similarly, the enzyme in the bulk phase is completely reduced by S. However, the enzyme is completely oxidized by the M_O generated at the electrode (Fig. 3C). Interestingly, the abundance ratio of the enzyme changes drastically in the reaction plane. This sharp change in the enzyme's redox state is due to the balance between the reduction by S and oxidation by M_O . This numerical simulation result demonstrates that the reaction plane assumed in the analytical model is appropriate.

The concentration profile of S seems to be spherical diffusion around the microelectrode, except in the region near the electrode. Figure 4A shows the concentration profiles of (solid line) S, (broken line) M_R , and (dotted line) E_R , along the rotation axis under conditions identical to those in Fig. 3. Additionally, the concentration profile of S in regions far from the electrode is shown in Fig 4B. The concentration gradient of M_R exists only inside the reaction plane, which is located at $z \simeq 3 \mu\text{m}$.

Interestingly, the profile of c_S has an inflection point on the reaction plane. The value of c_S inside the reaction plane is quite small (ideally, it will be zero), and the gradient of c_S at the electrode surface is nearly zero. These findings imply that the diffusion of S inside the reaction plane is negligible when $c_S(r_1) \ll c_S^0$.

When $c_S^0 = 5.0, 10,$ and 15 mmol dm^{-3} , the values of c_S on the reaction plane are 0.25, 0.9, and 2.0 mmol dm^{-3} , re-

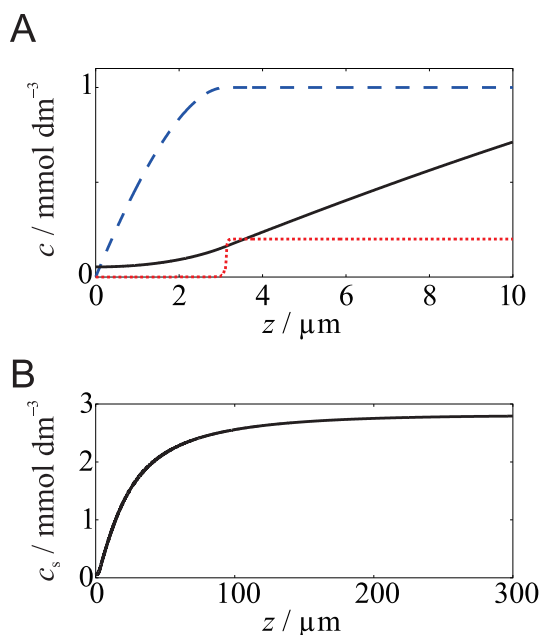


Fig. 4 (A) Concentration profiles of substrate (S) (solid line), reduced form of mediator (M_R) (broken line), and reduced form of enzyme (E_R) (dotted line) along rotation axis. (B) Concentration profile of substrate far from the electrode is shown as well. The profiles are recorded 20 s after the potential step. The simulated conditions are the same as those in Fig. 3.

spectively. The values indicate that the enzymatic reaction is almost completed inside the reaction plane, but not perfectly.

Here, for discussing the numerical simulation on the basis of the analytical model, the reaction plane in Fig. 3 is defined at the position of $c_{E_R} = c_E^0/2$. In addition, the radius of the reaction plane in the simulated result is determined using the radius of a hemisphere with the same surface area as the reaction plane.

4.3 Effect of the concentration on the current

The relationship between I_{20} and c_S is shown in Fig. 5 by triangles. The line in Fig. 5 shows the diffusion-controlled current calculated using eq. 21 at $D = 6 \times 10^{-10} \text{ m}^2 \text{ s}^{-1}$ and $c_b = c_S^0 - c_M^0 - c_E^0$. When the substrate concentration is low ($c_S^0 < 5 \text{ mmol dm}^{-3}$), I_{20} is close to the line. This agreement indicates that the conversion of the flow J_S to J_M is almost complete. Therefore, the microdisc electrode conjugated with the enzymatic reaction acts as an amperometric biosensor that detects steady-state mass flow of the substrate.

When c_S^0 is higher than 5 mmol dm^{-3} , the simulated current is deviated downward from the line representing the diffusion-controlled mechanism. Under these conditions, c_S at the electrode surface is far from zero, and it strongly depends on c_S^0 .

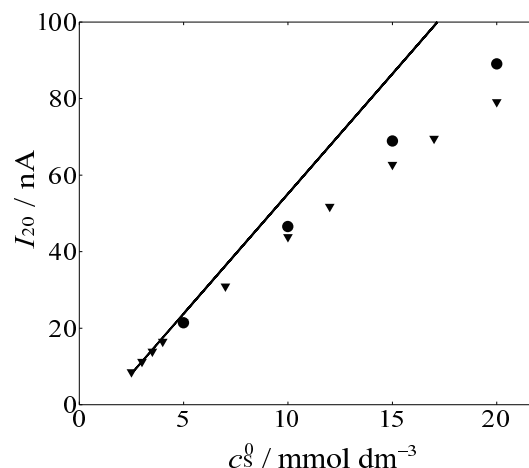


Fig. 5 Dependence of the steady-state current on the initial substrate concentration at $D_S = 6 \times 10^{-10} \text{ m}^2 \text{ s}^{-1}$, $D_M = 1 \times 10^{-10} \text{ m}^2 \text{ s}^{-1}$, $c_M^0 = 1 \text{ mmol dm}^{-3}$, and $c_E^0 =$ (triangles) 0.2 and (circles) 0.4 mmol dm^{-3} . The line shows the current calculated using eq. 21.

For accelerating the enzymatic reaction, c_E^0 is increased. The circles in Fig. 5 are I_{20} values calculated at $c_E^0 = 0.4 \text{ mmol dm}^{-3}$. Although the currents increase, the increments do not increase the current to values close to the diffusion-controlled values. This shows that the effect of c_E^0 on the linear range is small. In practical applications, decreasing the diffusion flux by increasing the viscosity may be necessary for expanding the linear range.¹²

Figure 6A shows the effect of c_{M_R} on the current. Although the value of c_{M_R} is changed from 0.2 to 2 mmol dm^{-3} , the change in I_{20} is smaller than 20 percent. This weak dependence of I_{20} on c_{M_R} is understood from the reaction plane position. The inset of Fig. 6A shows the dependence of r_1 on c_{M_R} . The horizontal dotted line in the inset of Fig. 6A represents the corresponding radius of the microdisc electrode (r_0). The value of $r_1 - r_0$ is proportional to the value of c_{M_R} . According to eq. 13, the current is proportional to $c_{M_R} r_1 / (r_1 - r_0)$. Given that the effect of c_{M_R} is canceled by $r_1 - r_0$, the weak dependence of I_{20} on c_{M_R} is ascribed to the insensitivity of r_1 on c_{M_R} . This result shows that the adjustment of c_M^0 does not have a high priority in amperometric biosensor optimization. The decrease in I_{20} at higher values of c_M^0 is related with the decrease of c_S in the bulk phase (eq. 14).

Figure 6B shows the effects of c_E^0 on I_{20} . When c_E is lower than 0.1 mmol dm^{-3} , I_{20} depends strongly on c_E^0 . Under these conditions, the current is controlled by the reaction rate of the enzymatic reaction. When c_E^0 is greater than 0.1 mmol dm^{-3} , I_{20} is independent of c_E^0 (the change in I_{20} over $c_E^0 = 0.1$ – 0.6 mmol dm^{-3} is less than 5 percent). This response reflects the ideal characteristic that the current is controlled by substrate diffusion when c_E^0 is sufficiently high. This concentration de-

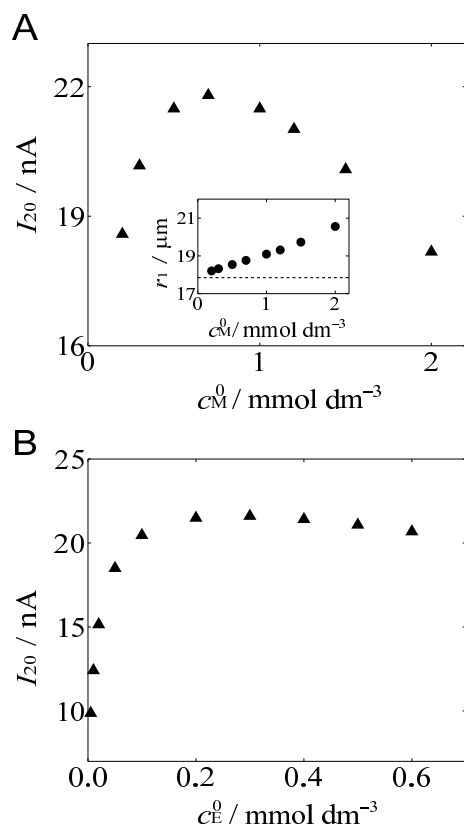


Fig. 6 Effect of initial concentration of (A) mediator and (B) enzyme on the current at $c_S^0 = 5 \text{ mmol dm}^{-3}$, (A) $c_E^0 = 0.2 \text{ mmol dm}^{-3}$, (B) $c_M^0 = 1 \text{ mmol dm}^{-3}$, $D_S = 6 \times 10^{-10} \text{ m}^2 \text{ s}^{-1}$, and $D_M = 1 \times 10^{-10} \text{ m}^2 \text{ s}^{-1}$. The inset of A shows the effect of c_M^0 on the corresponding reaction plane radius. The dotted line in the inset of A indicates the corresponding radius of the microdisc electrode's surface.

pendence is important for constructing amperometric biosensors, because the response in our method is independent of the enzyme activity as long as excess amounts of the enzyme exist.

In summary, the enzymatic microelectrode is sensitive to c_S^0 , but insensitive to c_E^0 and c_M^0 . The necessary condition for ensuring these enzymatic microelectrode characteristics is the excess enzyme activity in the solution phase.

4.4 Effect of the diffusion coefficients on the current

Figure 7A shows the dependence of I_{20} on D_S . The current increased with the increase of D_S . The line in Fig. 7A is the diffusion-limited current calculated from eq. 21. For small values of D_S , the simulated current agreed with the diffusion-limited current. However, the simulated current deviated downward from the line at higher values of D_S . The

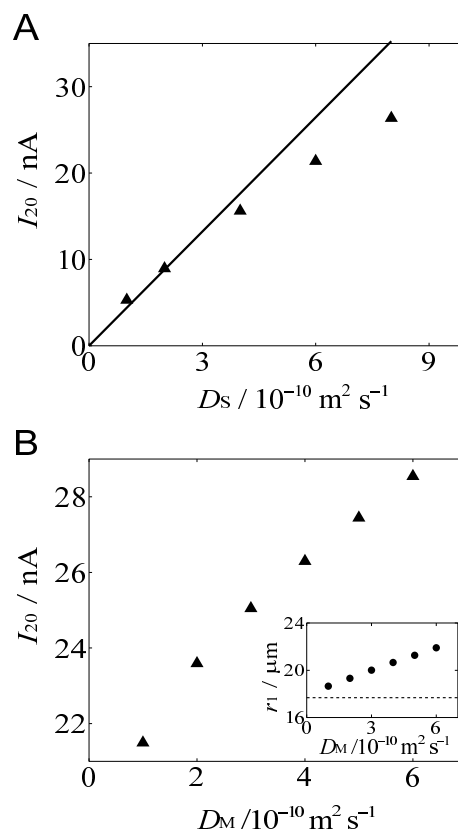


Fig. 7 Effect of diffusion coefficient of (A) substrate and (B) the mediator on the current at $c_S^0 = 5 \text{ mmol dm}^{-3}$, $c_M^0 = 1 \text{ mmol dm}^{-3}$, $c_E^0 = 0.2 \text{ mmol dm}^{-3}$, (A) $D_M = 1 \times 10^{-10} \text{ m}^2 \text{ s}^{-1}$, and (B) $D_S = 6 \times 10^{-10} \text{ m}^2 \text{ s}^{-1}$. The line in A shows the diffusion-limited current. Inset in B shows the effect of D_M on the corresponding radius of the reaction. Dotted line in the inset indicates the corresponding radius for the surface of the microdisc electrode.

limitation of the enzymatic reaction rate may cause this deviation, since J_S increases with an increase of D_S . When the value of D_S is high, J_S will exceed the reaction rate of the conversion from S to M_R .

Figure 7B shows the dependence of D_M on the current. The current increases as D_M increases. However, the current is insensitive to changes in D_M . This insensitivity is explained by the expansion of the reaction plane with an increase in D_M . The inset of Fig. 7B shows the relationship between r_1 and D_M , and a linear relationship between r_1 and D_M is obtained. According to eq. 13, I_{20} is proportional to $D_M r_0 r_1 / (r_1 - r_0)$. Given that the value of $D_M / (r_1 - r_0)$ remains almost constant (Fig. 7B), the small dependence of I_{20} on D_M is due to the insensitivity of r_1 to D_M . These features are effective from the application viewpoint because the current is independent of the selection of mediator. A mediator suitable for this sensor type is selected based on its standard potential and reactivity

with the electrode.¹⁹

When $c_S^0 < c_M^0$, this system became the endpoint analysis¹¹. In this situation, the current is determined by the diffusion of M_R . Therefore, the calibration curve of I_{20} will have an inflection point at $c_S^0 = c_E^0 + c_M^0$. To avoid this inflection point, D_S must be close to D_M .

4.5 Conclusions

When the enzymatic reaction is sufficiently fast, the enzymatic reaction-microdisc electrode combination provides a steady-state current controlled by substrate diffusion. The steady-state current is proportional to the concentration and the diffusion coefficient of substrate because the substrate flow completely converts to mediator flow at the reaction plane. The concentration and diffusion coefficient of mediator have limited effects on the steady-state current (as long as fast enzyme kinetics is guaranteed), because the change in the reaction plane position cancels the changes in the current values ascribed to the mediator characteristics. In addition, at sufficiently high levels of the enzyme activity, the steady-state current becomes independent of the enzyme activity. The use of the microelectrode allows the system miniaturization^{8,9} and the use of concentrated enzyme. Therefore, such an enzymatic electrode reaction on the microdisc electrode with fast enzyme kinetics becomes very useful for the miniaturized amperometric biosensor in future.

Acknowledgement

This work was supported in part by the Japan Science and Technology Agency, Crest (to M. Y.).

References

- 1 S. Tsujimura, S. Kojima, T. Ikeda and K. Kano, *Anal. Bioanal. Chem.*, 2006, **386**, 645–651.
- 2 J. Wang, *Chem. Rev.*, 2008, **108**, 814–825.
- 3 A. Heller and B. Feldman, *Chem. Rev.*, 2008, **108**, 2482–2505.
- 4 B. J. Privett, J. H. Shin and M. H. Schoenfish, *Anal. Chem.*, 2010, **82**, 4723–4741.
- 5 S. Borgmann, A. Schulte, S. Neugebauer and W. Schuhmann, in *Amperometric Biosensors*, ed. R. C. Alkire, D. M. Kolb and J. Lipkowski, Wiley-VCH Verlag GmbH Co. KGaA, Weinheim, Germany, 2011, ch. 1, pp. 1–83.
- 6 A. M. Bond, K. B. Oldham and C. G. Zoski, *Anal. Chim. Acta*, 1989, **216**, 177–230.
- 7 R. J. Forster, *Chem. Soc. Rev.*, 1994, **23**, 289–297.
- 8 S. F. Peteu, D. Emerson and R. M. Worden, *Biosens. Bioelectron.*, 1996, **11**, 1059–1071.
- 9 F. Tian, A. V. Gourine, R. T. R. Huckstepp and N. Dale, *Anal. Chim. Acta*, 2009, **645**, 86–91.
- 10 R. Matsumoto, K. Kano and T. Ikeda, *J. Electroanal. Chem.*, 2002, **535**, 37–40.
- 11 T. Noda, K. Hamamoto, M. Tsutsumi, S. Tsujimura, O. Shirai and K. Kano, *Electrochem. Commun.*, 2010, **12**, 839–842.
- 12 T. Noda, M. Wanibuchi, Y. Kitazumi, S. Tsujimura, O. Shirai, M. Yamamoto and K. Kano, *Anal. Sci.*, 2013, **29**, 279–281.
- 13 J. Galceran, S. L. Taylor and P. N. Bartlett, *J. Electroanal. Chem.*, 2001, **506**, 65–81.
- 14 A. Eswari and L. Rajendran, *J. Electroanal. Chem.*, 2010, **641**, 35–44.
- 15 A. Eswari and L. Rajendran, *J. Electroanal. Chem.*, 2011, **651**, 173–184.
- 16 S. Tsujimura, S. Kojima, K. Kano, T. Ikeda, M. Sato, H. Sanada and H. Omura, *Biosci. Biotechnol. Biochem.*, 2006, **70**, 654–659.
- 17 D. Shoup and A. Szabo, *J. Electroanal. Chem.*, 1982, **140**, 237–245.
- 18 Y. Saito, *Rev. Polarogr.*, 1968, **15**, 177–187.
- 19 K. Kano and T. Ikeda, *Anal. Sci.*, 2000, **16**, 1013–1021.